Int J Appl Earth Obs Geoinformation 89 (2020) 102113

Contents lists available at ScienceDirect

Int J Appl Earth Obs Geoinformation

journal homepage: www.elsevier.com/locate/jag

Retrieving soil moisture in rainfed and irrigated fields using Sentinel-2 observations and a modified OPTRAM approach

Mariapaola Ambrosone[a,1], Alessandro Matese[a,1], Salvatore Filippo Di Gennaro[a,*], Beniamino Gioli[a], Marin Tudoroiu[b], Lorenzo Genesio[a], Franco Miglietta[a], Silvia Baronti[a], Anita Maienza[a], Fabrizio Ungaro[a], Piero Toscano[a]

[a] Institute of BioEconomy (IBE), National Research Council (CNR), Via Caproni 8, 50145 Florence, Italy
[b] European Space Agency (ESA), ESTEC, Keplerlaan 1, 2200 AG, Noordwijk, the Netherlands

ARTICLE INFO

Keywords:
Soil moisture
Sentinel-2
Rainfed
Irrigated
Maize
Pasture

ABSTRACT

Surface soil water content plays an important role in driving the exchange of latent and sensible heat between the atmosphere and land surface through transpiration and evaporation processes, regulating key physiological processes affecting plants growth. Given the high impact of water scarcity on yields, and of irrigated agriculture on the overall withdrawal rate of freshwater, it is important to define models that help to improve water resources management for agricultural purposes, and to optimize rainfed crop yield. Recent advances in satellite-based remote sensing have led to valuable solutions to estimate soil water content based on microwave or optical/thermal-infrared data. This study aims at improving soil water content estimation at high spatial and temporal resolution, by means of the Optical Trapezoid Model (OPTRAM) driven by Copernicus Sentinel-2 data. Two different model variations were considered, based on linear and nonlinear parameters constraints, and validated against *in situ* soil water content measurements made with time domain reflectometry (TDR) on irrigated maize in central Italy and on rainfed maize and pasture in northern Italy. For the first site the non-linear model shows a better correlation between measured and estimated soil water content values (r = 0.80) compared to the linear model (r = 0.73). In both cases the modeled soil moisture tends to overestimate the measured values at medium to high water content level, while both models underestimate soil moisture at low water content level. Estimated versus measured normalized surface soil water for rainfed pasture plots from nonlinear OPTRAM parametrized based on irrigated maize parameterization (SIM1), and site-specific parametrization for rainfed pasture (SIM2), indicate that both models (SIM1 and SIM2) are comparable for rotational grazing pasture (RMSEsim1 = 0.0581 vs. RMSEsim2 = 0.0485 cm3 cm-3) and the continuous grazing pasture (RMSEsim1 = 0.0485 vs. RMSEsim2 = 0.0602 cm3 cm-3), while for the rainfed maize plots SIM1 shows lower RMSE (average for all plots RMSE = 0.0542 cm3 cm-3) compared to the site-specific calibration model (SIM2 – average for all plots RMSE = 0.0645 cm3 cm-3). Finally, OPTRAM estimations are close to *in situ* measurement values while Surface Soil Moisture at 1 km (SSM1 km) tends to underestimate the measurements during maize crop growing season. Soil moisture retrieval from high-resolution Sentinel-2 optical images allows water stress conditions to be effectively mapped, supporting decision making in irrigation scheduling and other crop management.

1. Introduction

Surface Soil Moisture (SSM) is a key variable related to the health of terrestrial ecosystems and specifically to agriculture crops. It supports water flow and transport processes in the soil-plant-atmosphere system (Campbell and Norman, 1988; Zhang and Zhou, 2016; Lakshmi, 2012), finally controlling latent heat flux to the atmosphere. SSM is defined as the temporary storage of rainfall in the top soil layer, called the aeration zone. This part of the soil profile is fundamental for agriculture since it controls the amount of water available to plant roots therefore it

* Corresponding author.
E-mail addresses: mariapambr@gmail.com (M. Ambrosone), alessandro.matese@cnr.it (A. Matese), salvatorefilippo.digennaro@cnr.it (S.F. Di Gennaro), beniamino.gioli@cnr.it (B. Gioli), marin.tudoroiu@esa.int (M. Tudoroiu), lorenzo.genesio@cnr.it (L. Genesio), franco.miglietta@cnr.it (F. Miglietta), silvia.baronti@cnr.it (S. Baronti), anita.maienza@cnr.it (A. Maienza), fabrizio.ungaro@cnr.it (F. Ungaro), piero.toscano@cnr.it (P. Toscano).
[1] The two authors contributed equally to this work.

https://doi.org/10.1016/j.jag.2020.102113
Received 27 November 2019; Received in revised form 6 March 2020; Accepted 9 March 2020

regulates the key physiological processes affecting growth (Lakshmi, 2012; Wang et al., 2007). SSM is very sensitive to changes in environmental conditions, since rising temperatures and current and expected changes in the global climate determine alterations in the hydrology and surface energy balance of entire landscapes (Vanino et al., 2018). This translates into changes of evapotranspiration and precipitation trends at different scales, resulting in unpredictable rainfall, drought events and water scarcity (IPCC, 2013; Avramova et al., 2016; Vanino et al., 2018). Changes in global temperature control the heat and water balance between the land surface and the atmosphere, which are fundamental in determining crop yield and efficiency of resource use in agriculture production (Tollenaar and Lee, 2002). Given the high impact that agricultural practices have on the overall withdrawal rate of freshwater (Lakhankar et al., 2009; WWAP, 2015), it is important to define models that help to improve both the management of water resources for agriculture, and the management of rainfed crops.

Soil moisture is highly variable in time and space due to heterogeneity of soil properties, topography, land cover and the non-uniformity of rainfall events and evapotranspiration rates at various spatial scales (Crow et al., 2012; Umar et al., 2016; Santos et al., 2014). Time domain reflectometry (TDR) or gravimetric sampling techniques can provide quantitatively accurate point based field measurements of soil moisture but they cannot consider changes in spatial distribution across gradients of soil surface characteristics (Lakhankar et al., 2009). The development of satellite technologies allowed to assess spatial-temporal variability with remote sensing, both optical and radar based, providing quantitative estimations of SSM from local up to global scale (Ahmed et al., 2011; Mulder et al., 2011). Earth Observation products were shown to be a valid tool for soil moisture retrieval, providing high temporal and spatial resolution data in support of real-time crop needs at both regional and global scale (Zhang and Zhou, 2016; Wang et al., 2007; Mulder et al., 2011).

This study focuses on the determination of SSM using Copernicus Sentinel-2 (S2) optical data to drive the recently proposed Optical Trapezoid Model (OPTRAM) (Sadeghi et al., 2017). Model accuracy was assessed through validation with *in situ* SSM measurements obtained in two study areas from northern and central Italy with the TDR technique. A nonlinear parameterization procedure was used in addition to the standard linear procedure to improve SSM retrieval accuracy. Finally, the values obtained here and based on optical data were compared with low-medium resolution (1 km) and high-frequency SSM products developed by Bauer-Marschallinger et al. (2018) and obtained through data fusion of Metop-ASCAT and Sentinel-1 available in the Copernicus Global Land Service (CGLS) (https://land.copernicus.eu/global/products/swi). This study is amongst those aiming to derive a universally valid SSM estimation model through optical remote sensing, finally providing reliable and accurate quantitative SSM data. The OPTRAM model was implemented in the Mediterranean environment to determine the applicability of a universal parameterization that accounts for different environmental and crop management conditions (rainfed and irrigated). Finally, the robustness of the methodology is critically assessed.

1.1. Conceptual framework

Advances in the technical capabilities of space-borne sensors opened the way to new in-depth studies on the application of RS to estimate and monitor SSM (Dash and Ogutu, 2016). When considering crop management, precise use of freshwater for irrigation purposes is essential for supporting sustainable and efficient practices in order to guarantee high crop yields (Lakhankar et al., 2009). Temporal and spatial monitoring of soil moisture throughout the growing stages of crops will prevent water stress and improve the overall crop performance (Vuolo et al., 2015; Doraiswamy et al., 2004). Remote sensors cannot directly measure SSM content, but instead use a proxy variable related to measured signals. This section provides an overview of the current state of the art in RS soil moisture estimation methods that allowed three main groups to be distinguished, based on the different sensors used (Kerr, 2007; Moran et al., 2004; De Ridder, 2000; Magagi et al., 2016).

1.1.1. Passive microwave sensing of SSM

Changes in SSM lead to changes in the surface emissivity detected with microwave frequency. The estimation of SSM using passive microwave sensors is based on the difference between the dielectric properties of water and of dry soil, measured as variations in the soil brightness temperature of dry and wet soils (Njoku and Kong, 1977). Microwave sensors are also used to measure emissivity in its different spectral windows. In the field of passive microwave sensors, e.g. the Advanced Microwave Scanning Radiometer (AMSR-E, Njoku et al., 2003; Koike et al., 2004; McCabe et al., 2005), Soil Moisture and Ocean Salinity (SMOS, Kerr et al., 2012), several algorithms were developed based on the use of different combinations of frequencies and polarizations as well as different type of ancillary data (Jackson, 1993; Njoku and Li, 1999; Owe et al., 2001; Paloscia et al., 2015). At the base of these algorithms is the physical based radiative transfer model (RTM), conceived to estimate SSM from the microwave signal based on assumptions of scattering albedo, vegetation roughness and surface temperature, e.g. SVAT-infrared thermal radiative transfer models by François (2002) (Gao et al., 2004, 2006; Dobson et al., 1985; Chauhan, 1997; Pan et al., 2014).

Despite the capability of passive microwave sensors to observe the earth's surface regardless of meteorological conditions, their coarse spatial resolution limits their application below the 10 km scale (Bauer-Marschallinger et al., 2018).

1.1.2. Active microwave sensing of SSM

Active sensors transmit information as a series of pulses while the radar antenna traverses the imaged landscape, which are then processed together to simulate a long aperture capable of providing high surface resolution scenes (Ulaby et al., 1996). The active sensor systems able to cover frequencies suitable for RS soil moisture estimations include Sentinel 1-A satellite, which provides C-band images (Şekertekin et al., 2016); C-band RADARSAT-1/2; Soil Moisture Active Passive (SMAP) missions (Chan et al., 2016); and ASCAT scatterometer onboard the Metop-A satellite (Wagner et al., 1999; Paulik et al., 2014). Radars represent a good source of data for SSM retrieval due to the higher spatial resolution when compared to radiometers but lack the capacity to discriminate signal interaction associated with measured backscatter data influenced by surface roughness, vegetation canopy and vegetation water content (Lakshmi, 2012). To overcome these limitations some models were conceived considering SAR and radiometer data fusion (Bauer-Marschallinger et al., 2018; He et al., 2014; Peng et al., 2017). An ideal SSM retrieval algorithm would combine the high spatial resolution of SAR with the high sensitivity of a radiometer to obtain an improved soil moisture product (Lakshmi, 2012). Bauer- Marschallinger et al. (2018) proposed a data fusion approach combining two different data sources, METOP-ASCAT and Sentinel-1, in order to calculate a Soil Water Index (SWI) providing data on a daily basis at 1-km spatial resolution.

1.1.3. Optical/thermal sensing of SSM

This method is based on the use of visible, short wave and thermal infrared optical bands (wavelengths ranging between 0.4 and 15 μm) to retrieve surface reflectance (Sobrino et al., 2012; Rahimzadeh and Berg, 2016). In the field of the optical/thermal imagery-based approach, the technique most applied for SM retrieval is based on a "triangular" or "trapezoidal" concept. The model, hereinafter called Thermal-Optical Trapezoid Model (TOTRAM) (Nemani et al., 1993; Carlson et al., 1994), is derived from the interpretation of the relationship existing between the pixel distribution of Land Surface Temperature (LST), and vegetation indices (VI) (Piles et al., 2011; Lambin and Ehrlich, 1996; Gillies

et al., 1997). Several modifications to the conventional trapezoid model were proposed to improve its accuracy. Two of the major limitations of the TOTRAM model are associated with the concomitant use of thermal and optical satellite data and the need for constant calibration/parametrization due to the variability of LST, which is easily influenced by near surface temperature, relative humidity and wind speed (Mallick et al., 2009). The conventional trapezoid model was thus replaced by an alternative model developed by Sadeghi et al. (2017) that replaces thermal bands with shortwave infrared bands that are simultaneously available on the same satellite. Despite the growing number of studies on RS based estimations of SSM at a global scale, numerous challenges derive from building a universally applicable model inclusive of all the parameters affecting surface soil moisture (Zhang and Zhou, 2016). Some of the current limitations are associated with: (i) the input parameters of SSM models; (ii) physical interpretation of different surface variables from satellite data and their discrimination; (iii) spatial and temporal resolution of the images acquired being influenced by surface roughness and vegetation cover; (iv) difficulties in establishing a universal relationship between SSM and soil texture across different study areas; (v) lack of surface data for validation of remotely sensed SSM that are given as single data points not considering the spatial and temporal variability of SSM over a given region (Bosch et al., 2006).

The OPTRAM model is presented in the next section. OPTRAM is a simple linear model at Short-wave Infra-Red (SWIR) wavelengths (0.7–2.5 μm), with physically definable parameters, offering a straightforward method for remote sensing SSM retrieval based on optical images (Sadeghi et al., 2015). The model was chosen for the feasibility of its implementation and the potential universal calibration of its parameters over heterogeneous soils.

1.1.4. Theoretical background: the optical TRApezoid model (OPTRAM)

OPTRAM relies on the use of optical data to retrieve SSM (Sadeghi et al., 2017). It explores the relationship between soil moisture in the root zone soil layer and vegetation dynamics represented by vegetation indeces. Soil water content (W) is derived by combining the normalized difference vegetation index (NDVI) as a measure of fraction of absorbed photosynthetically active radiation and shortwave infrared (SWIR) transformed reflectance (STR) values (Sadeghi et al., 2015). These indeces are a measure of the health and vigor of vegetation that is dependent, amongst other factors, on the soil water content (Liu et al., 2012). Soil water status influences vegetation growth and changes in soil water content will result in changes to the spectral characteristics of vegetation (Chen et al., 2014; Santos et al., 2014). The assumption of the existence of a linear relationship between soil and vegetation water content, is built upon the theory of reflectance and developed into a simple regression model (Sadeghi et al., 2015).

OPTRAM was developed based on the Kubelka and Munk (1931) theory of reflectance describing a two-flux radiative transfer (a downward and an upward light propagation flux, *I* and *J*) in an absorbing and scattering layer (Sadeghi et al., 2015). The model is built on two differential equations putting in relation the radiance, *I* and *J,* at a depth in the layer *z* at a given wavelength and with a light absorption (*k)* and a light scattering coefficient (*s*). The reflectance (R) is obtained as a function of *k* and *s*.

$$R = 1 + \frac{k}{s} - \sqrt{\left(\frac{k}{s}\right)^2 + 2\frac{k}{s}} \quad (1)$$

The SWIR transformed reflectance is then derived as follows when considering R at the SWIR bands:

$$STR = \frac{k}{s} = \frac{(1 - R^2)}{2R} \quad (2)$$

Assuming the existence of a linear relationship between soil saturation degree and STR, W results in:

$$W = \frac{STR_d - STR}{STR_d - STR_w} \quad (3)$$

where STR*d* and STR*w* are the STR values at dry and wet conditions and R is surface reflectance for the SWIR band. Assuming a linear relationship between soil water content and vegetation water content, the dry and wet edges of the theoretical trapezoid formed between the STR-NDVI spaces are defined as follows:

$$STR_d = i_d + s_d \times NDVI \quad (4)$$

$$STR_w = i_w + s_w \times NDVI \quad (5)$$

where i_d and s_d are the intercept and the slope of the dry edge and i_w and s_w the intercept and the slope of the wet edge. The NDVI vegetation index is defined as the difference in amplitude between the red and near infrared (NIR) regions (Deering, 1979):

$$NDVI = \frac{R_{NIR} - R_{RED}}{R_{NIR} + R_{RED}} \quad (6)$$

2. Materials and methods

2.1. Study areas

2.1.1. Northern italy - Trentino, rainfed maize and rainfed pasture

AgriLife farm (www.agrilife.bio) is an organic dairy farm, located in Comano Terme in Trentino Alto Adige region (46°00′10.44″ N 10°52′12.88″ E; elev. 508 m a.m.s.l.), raising donkeys that graze outdoors. Soil water was monitored at 3 dates in 2018 on two pastures that are managed with two different grazing systems: continuous and rotational (PC and PT respectively, Fig. 1a right panel, Table1). Continuous grazing implies that animals graze continuously on a single pasture for the entire growing season (from May to October), while rotational grazing permits the recovery and growth of the pasture. Three measurement points were identified for each pasture, at a 10-m distance from each other for PC (PC1, PC2, PC3, Table 1) and 30-m for PT (PT1, PT2, PT3, Table1).

Cargos farm is a conventional farm located in Fiavè in Trentino Alto Adige region (45°59′22.77″ N 10°50′03.03″ E; elev. 655 m a.m.s.l.), growing rainfed maize for silage (Fig. 1a left panel). Soil water was monitored at 3 dates in 2018 in two points (at 20-m distance from each other) for each of the four areas selected in the maize field (C1, C2, MA, MB, Fig. 1a left panel, Table1)

Both sites are located in a glacial plain on glacial deposits covered by heterogeneous croplands; dominant soils are classified as Cutanic Luvisols, coarse loamy (IUSS, 2015), formed on Tertiary limestone and Mesozoic dolomite, and on Holocenic alluvial deposits. Average annual temperature is 10.1 °C; average rainfall 834 mm. At both sites surface soil water content was measured with a soil water sensor (Delta-T Devices SM150 T). The measurement was made at 0 − 15 cm depth pushing the sensor into the soil until the rod was fully inserted ensuring good soil contact.

2.1.2. Central Italy - Tuscany, irrigated maize

The experimental site of Tuscany-Grosseto (42°49′47.02″ N 11°04′10.27″ E; elev. 2 m a.m.s.l.) is located in central Italy 20 km away from central Tuscany coastline (Fig. 1b). Average annual temperature is 15 °C and average annual rainfall is 640 mm. The site is part of a dairy farm (Azienda Agricola Le Rogaie). It mainly consists of a large flat irrigated area extending over 72 ha where maize was cropped during summer 2018. The area has a circular shape with 1 km diameter and is irrigated by a rotating pivot-irrigation system, which normally operates 24 h a day in the period June-August. A full irrigation cycle is completed within 4 days.

The predominant soils are classified as Eutric Vertisols, fine silty (IUSS, 2015), formed on substrates consisting of reclamation deposits and recent alluvial deposits. Soil volumetric water content data were

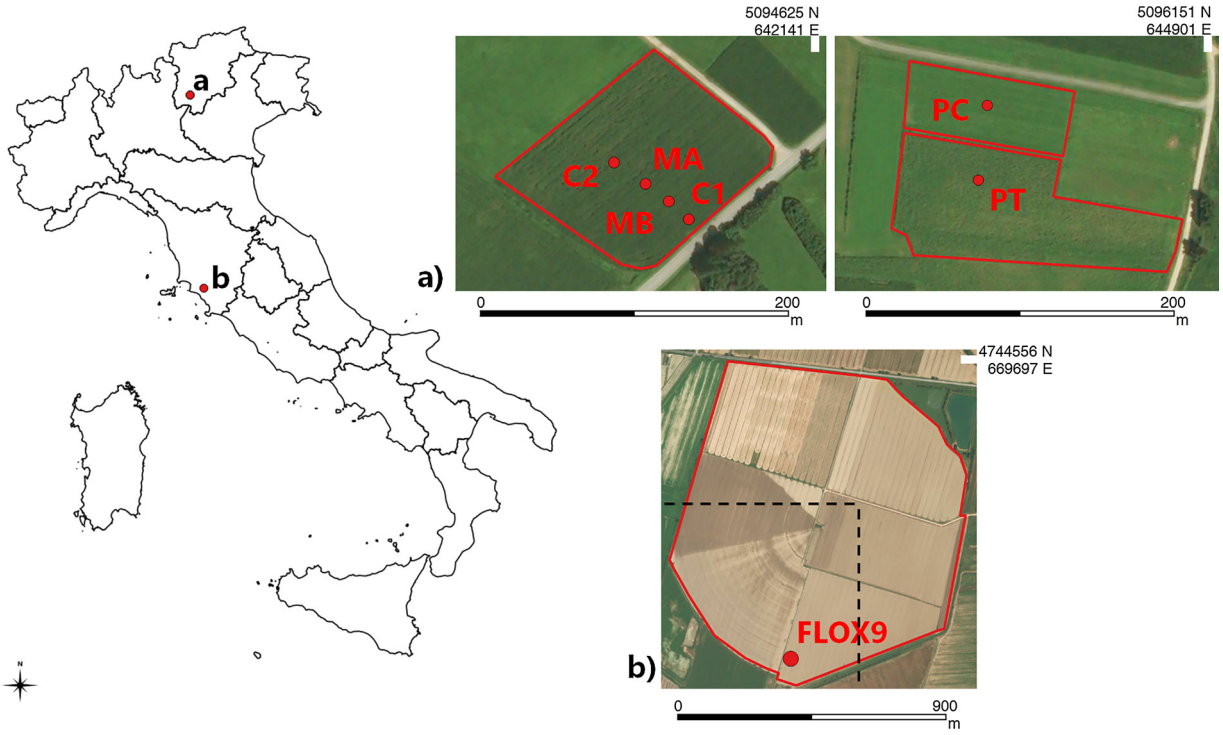

Fig. 1. Study area: a) Trentino Alto Adige region (case study Cargos and Agrilife farms), b) Tuscany region case study (red line irrigated maize field, dashed black line superimposed SSM1 km pixel).

Table 1
Details of study areas and satellite images.

	Location (UTM 32 N)	ID	Crop	Sentinel-2 acquisition date/ Ground measurements dates
Tuscany - Grosseto	4743984 N 669179 E	Flox9	Irrigated maize	2018 (Jul. 8, Jul. 13, Jul. 18, Aug. 2, Aug. 12, Aug. 17, Aug. 22, Aug. 27, Sept. 6, Sep. 11) / Jul.1- Sept.31
Trentino- Cargos	5094544 N 642072 E	C2A C2B ML2B ML1B C1B C1A ML2A ML1A	Rainfed Maize	2018 (Jul. 18, Sept. 11, Oct. 19) / (Jul. 19, Sept. 13, Oct. 18)
Trentino - Agrilife	5096059 N 644798 E	PT1 PT2 PT3 PC1 PC2 PC3	Rainfed Pasture	2018 (Jul. 18, Sept. 11, Oct. 19) / (Jul. 19, Sept. 13, Oct. 18)

measured at one location point (FLOX 9, Fig. 1b, Table1) by means of C650 TDR (Campbell Scientific, Logan, UT, USA) and acquired with a CR3000 data logger (Campbell Scientific, Logan, UT, USA) at 5 min intervals at 0 – 30 cm depth. The TDR was continuously operated from the beginning of July till end of September; no data are available for the period 12–18 July due to a datalogger failure in saving data.

2.2. Remote sensing data

2.2.1. Sentinel 2

Multispectral ESA Sentinel-2A and 2B satellite images providing 13 spectral bands covering the visible, NIR and SWIR at 10, 20 and 60 m spatial resolution were retrieved from ESA Sentinel Scientific Data Hub (https://copernicus.eu/) for the same day or the day following the in situ soil water measurement for each location. Sentinel-2 images were atmospherically corrected using the Sen2Cor algorithm (http://step.esa.int/main/third-party-plugins-2/sen2cor), which processes ESA's Level-1C top-of-atmosphere reflectance to atmospherically-corrected bottom-of-atmosphere (BoA) reflectance (Level-2A). Polygons corresponding to the study areas were extracted from each of the Sentinel-2 images. Reflectance values from bands 4 (red) and 8 (near infrared) were used to calculate NDVI and the reflectance from band 12 (SWIR) was used for calculating STR. Band 12 images at 20-m spatial resolution were resampled at 10-m with the nearest neighbor method to match the spatial resolution of bands 4 and 8. For the period of interest 13 cloud-free scenes were obtained: 10 for Tuscany and 3 for Trentino (Table 1). Though only a limited number of cloud-free images were available to match the exact dates of *in situ* measurements, the collected images enabled a complete temporal coverage of the *in situ* measuring dates.

2.3. OPTRAM parameterization

OPTRAM was parameterized based on the pixel distribution within the STR-NDVI space for the Tuscany case study. Two scenarios were considered, one based on OPTRAM linear model and the second on the use of a nonlinear OPTRAM model. The dry and wet edges of the model were determined based on the pixel distribution within the STR-NDVI space (Fig. 2a). For the first scenario the dry (i_d and s_d) and wet (i_w and s_w) edges parameters were determined by means of a linear fit of the STR-NDVI point cloud. In accordance with Sadeghi et al. (2017), fitting the edges was done based on visual inspection. The normalized soil water content (W) for each pixel was estimated from the dry edge and wet edge parameters via the use of equations and parameters reported in Fig. 2a.

Since the STR-NDVI scatterplots showed non-linear trends in the dry and wet edges, for the second scenario we considered the use of a nonlinear OPTRAM model. The dry (i_d and s_d) and wet (i_w and s_w) edges parameters were modeled by an exponential function that is a nonlinear combination of the model parameters depending on the STR and NDVI pixel distribution:

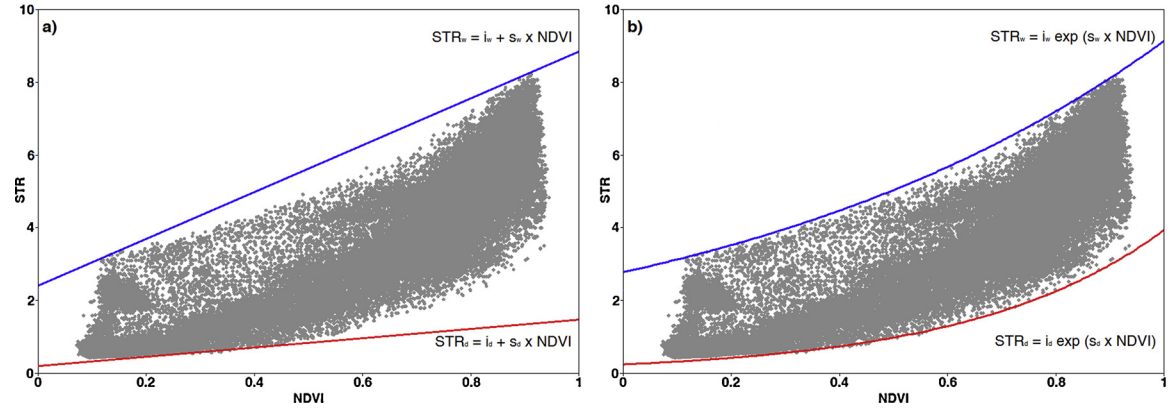

Fig. 2. Pixel distribution within the STR-NDVI space for the linear (a) and nonlinear OPTRAM in the Tuscany region (b). STR_d (dry – solid red line) and STR_w (wet – solid blue line) were reported for both models (linear and non-linear).

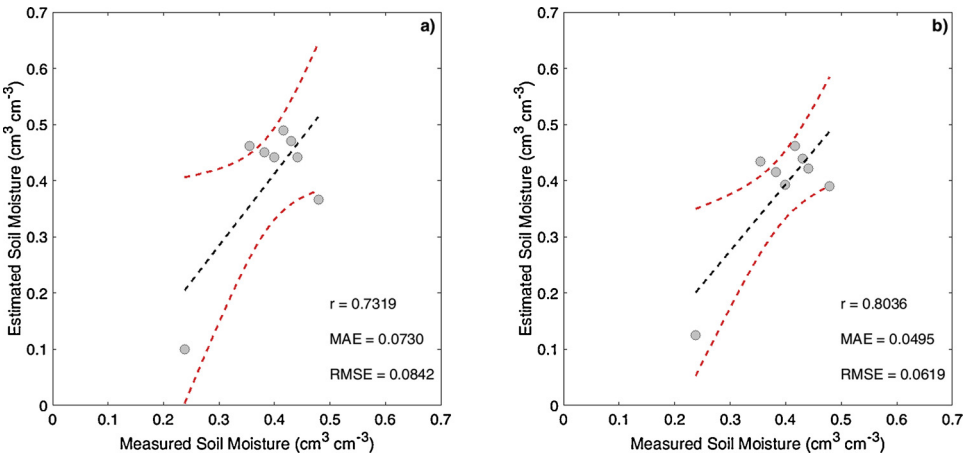

Fig. 3. Linear (a) and nonlinear (b) OPTRAM soil moisture estimates compared to in situ soil moisture measurements from the Flox9 measurement point (Tuscany case study).

$$STR_d = i_d \exp(s_d \times NDVI) \quad (7)$$

$$STR_w = i_w \exp(s_w \times NDVI) \quad (8)$$

W values for each pixel were then computed using Eq. (3) based on dry and wet edges parameters via Eq.s (7) and (8) (Fig. 2b).

$$W = \frac{i_d \exp(s_d \times NDVI) - STR}{i_d \exp(s_d \times NDVI) - i_w \exp(s_w \times NDVI)} \quad (9)$$

The OPTRAM model aims at obtaining a universal parameterization suitable for different areas, provided that a broad range of soil moisture and NDVI is obtained within a single scene to constrain such parametrization (Babaeian et al., 2019). In order to test the accuracy of a single calibration for all the study areas, the non-linear dry and wet edges parameters of the Tuscany-Grosseto site were then used for the estimation of W values for the Cargos and Agrilife farms in Trentino region (SIM1). A site-specific calibration for Cargos and Agrilife farms in Trentino region was also computed in order to compare the results of the two calibrations and verify to what extent a universal parameterization could be representative of the heterogeneous soil conditions over different regions and for different crop management (SIM2).

Model implementation and soil water content maps creation were created using R (R Core Team 2019, https://www.r-project.org/).

2.4. SSM 1 km product from Scatterometer and SAR data fusion

The SSM estimations derived from OPTRAM model were also compared with a low-medium resolution (1 km) and high temporal frequency SSM products developed by Bauer-Marschallinger et al. (2018) in order to compare the accuracy and performance of different RS soil water retrieval techniques for Tuscany region case study. SSM data was obtained from Copernicus Global Land Services database (https://land.copernicus.eu/global/). A total of 24 scenes were downloaded over the study area from July 6th to September 20th 2018. The whole study area is covered by 4 SSM 1 × 1 km pixels; the pixel with the highest cover percentage (about 40 %, Fig1b) and including the Flox 9 measurement point was selected, extracted and processed. SSM 1 km data were lastly compared against soil water content measurement, on a daily basis, and OPTRAM SM was calculated for the overlapping area. For a complete analysis daily rainfall collected by a rain gauge were also reported. Data extraction and analysis were performed using Matlab (Mathworks Inc. 2016).

3. Results and discussion

3.1. Tuscany case study – linear vs. Nonlinear model

A comparison of the OPTRAM SM estimates with *in situ* measurements is depicted in Fig. 3, showing the performance of both linear and nonlinear model calibrations. Albeit 10 Sentinel-2 passages were available (Table 1) for the entire study period, *in situ* data for two dates (July 13 and July 18) were not available due to a logging system failure. The nonlinear model shows a better correlation between measured and estimated soil water content values (r = 0.80) compared to the linear model (r = 0.73) (Fig. 3). RMSE was also lower (0.0619 $cm^3\ cm^{-3}$) for the nonlinear compared to the linear model (0.0842 $cm^3\ cm^{-3}$), and the same result was obtained with MAE (Mean

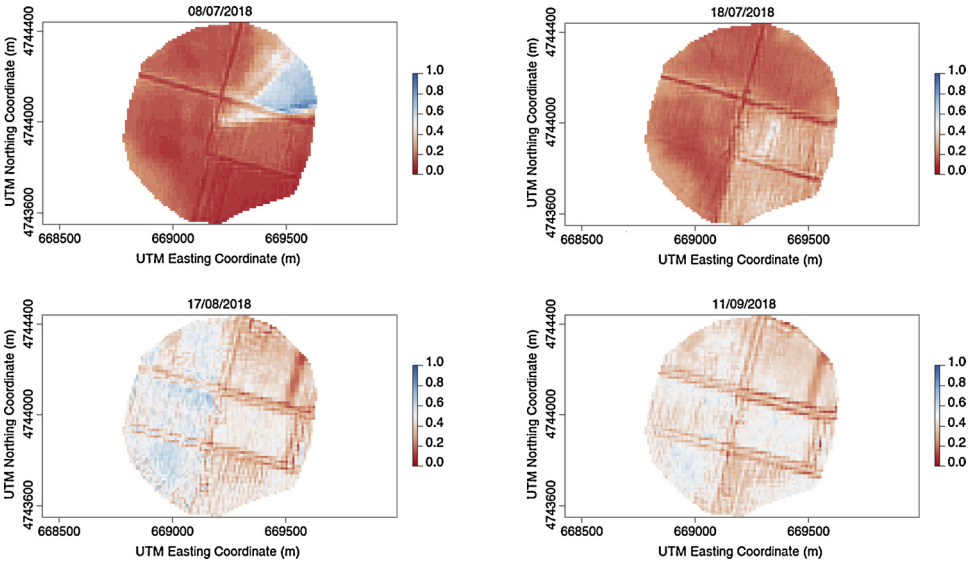

Fig. 4. Tuscany case study soil moisture maps obtained with nonlinear model.

Absolute Error) ranging from 0.073 (linear model) to 0.049 (exponential model) $cm^3\,cm^{-3}$. In both cases the modeled SM tends to overestimate the measured values at medium to high water content level, while both models underestimate SM at low water content level. Both the underestimation and overestimation are reduced when using the non-linear parameterization model. In fact, whereas OPTRAM linear and nonlinear parameterization give a yield resembling overall accuracy, the nonlinear model provides a better estimation of the real SM for the Tuscany case study.

Comparing the values of *in situ* SM with those modeled with OPTRAM, the estimation errors for both models are within the range of what was described as reasonable agreement accuracy for remote sensing mapping of SM (Sadeghi et al., 2017; Babaeian et al., 2018; Mananze et al., 2019) when using OPTRAM parameterization based on Landsat 8, Sentinel 2 or MODIS observations.

Soil Moisture maps generated from OPTRAM non linear parameterization are shown in Fig. 4. Within the whole period, 4 dates were selected in order to cover the temporal variability of soil moisture. Date-by-date visual comparison of the images shows that the model was able to capture temporal and spatial variation of soil water underlying the physically based relationship existing between volumetric soil moisture and SWIR reflectance of bare or vegetated soils (Sadeghi et al., 2015).

Moreover SM maps highlight the capability of the nonlinear model in mapping moisture spatial variability at fine scale, especially on August 17th September 11th, where spatial features of soil moisture deriving from different fields and from the pivot irrigation management are clearly detected. A very low moisture condition is mapped on July 8th, the driest date of the whole period both in models and measurements (0.09, 0.12, 0.23 cm3 cm-3 for linear, nonlinear and measurement respectively) as highlighted in Fig. 3.

3.2. Evaluation of OPTRAM estimations for the Trentino area

The soil moisture estimations using a site-specific nonlinear calibration (SIM2) were compared to those obtained using the parameterization from the Tuscany case study (SIM1), for both Trentino sites (Agrilife and Cargos). For the rainfed pastures (Agrilife) the results indicate that both models (SIM1 and SIM2) are comparable (Fig. 6). In the case of the rotational grazing pasture (PT), a slight improvement in terms of coefficient of correlation and RMSE is achieved with the site-specific nonlinear calibration (SIM2), while MAE slightly increased (0.0397 vs. 0.0401 $cm^3\,cm^{-3}$). Similar results are obtained for the continuous grazing pasture (PC). In this case using the model based on local calibration leads to a higher correlation, but at the same time to an increase in RMSE and MAE (0.0485 vs. 0.0602 $cm^3\,cm^{-3}$ for RMSE and 0.0404 vs. 0.0533 $cm^3\,cm^{-3}$ for MAE).

The implementation of OPTRAM using only optical remote sensing data for irrigated maize in Tuscany region produced realistic soil moisture values for the pasture in Trentino region. A local calibration led to higher correlation coefficients, but similar or worse RMSE and MAE values (Fig. 5). Although the errors are comparable with those observed for irrigated maize (Tuscany case study, RMSE < 0.06 $cm^3\,cm^{-3}$), a worse performance of both models for pastures is evident in terms of correlations.

It is worth to note that for this case study we evaluated the spatiotemporal distribution of SM represented by 3 points of measurement within 20 m for PC and within 60 m for PT. It should also be noted that the value of STR, for SM estimation, was calculated on the basis of S2 band 12, which has a native resolution of 20 m, and then resampled at 10 m.

Multiple studies report good results in soil water retrieval from radar imagery at the watershed scale. On the contrary, few report similar results at field or site scale level (Thoma et al., 2008). Thoma et al. (2008) confirmed the spatial limitation of high-resolution radar imagery for estimating field scale SM, indicating 35 m as the optimal resolution for watershed averaged estimates of soil moisture (filtered images) and > 150 m for unfiltered images. He et al. (2014) developed a methodology describing the use of microwave/optical data for soil moisture retrieval in an alpine prairie. Their research, based on an Integral Equation Method, a Water Cloud Model and an inversion scheme for soil water retrieval, achieved better results than our OPTRAM results for pasture (higher coefficient of correlation with similar RMSE) despite having a lower resolution (30 m) and not accounting for temporal analysis (one date).

Similarly, the exponential model implemented for the Tuscany case study, and the site-specific calibration for Trentino region were tested against soil water measurements for the Cargos farm site (rainfed maize). The nonlinear Tuscany model (SIM 1, Fig. 6 a, b, c, d) shows lower RMSE and MAE values compared to the site-specific calibration model (SIM2 Fig. 6e, f, g, h), except for C1A-C1B field area. In general, site-specific calibration for all field areas led to higher Pearson correlation coefficient, although a slight deterioration of relative and absolute errors was observed. This slight increase in the relative and absolute errors could be attributed to the higher number of data used (over an area of 72 ha) to implement the model for the Tuscany case study if

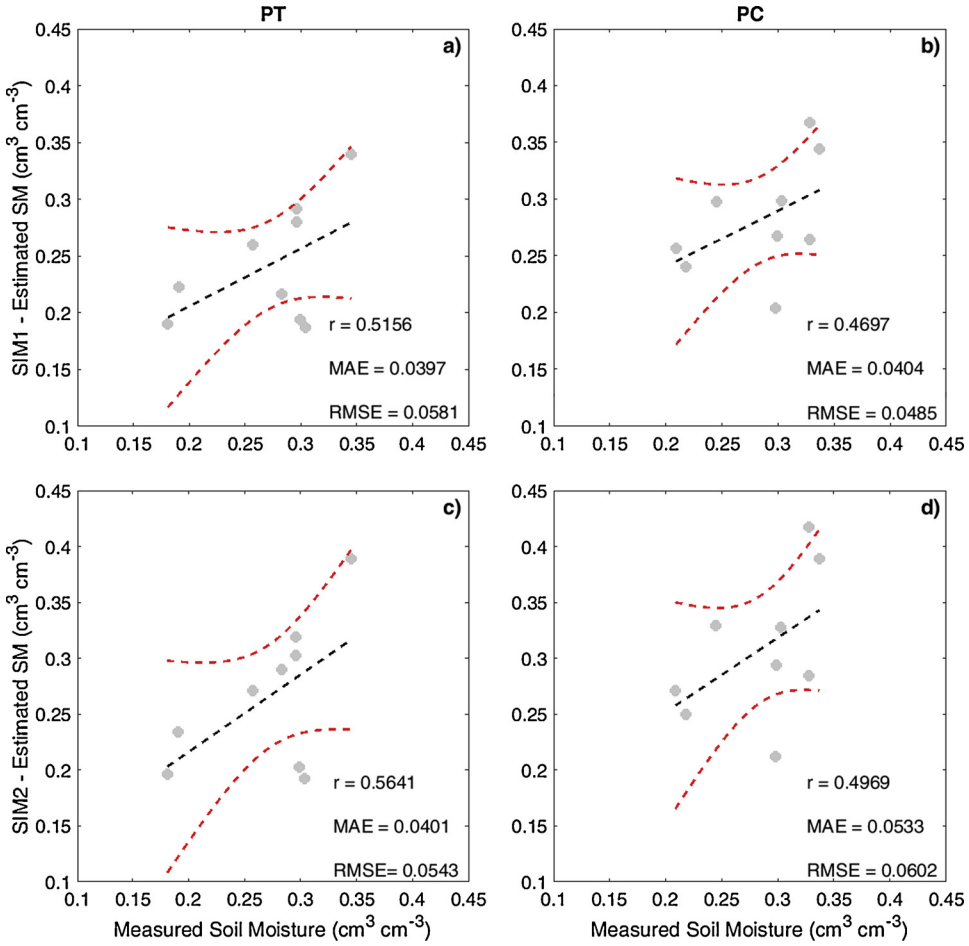

Fig. 5. Estimated versus measured normalized surface soil water for Agrilife plots from nonlinear OPTRAM parametrized based on Tuscany region parameterization (a and b, SIM1), and site-specific parametrization for Trentino region (c and d, SIM2) for rainfed rotational grazing pasture (PT) and rainfed continuous grazing pasture (PC).

compared to the site-specific model tested on the two case studies for the Trentino region (over an area of 1 ha for Cargos and 1.5 ha for Agrilife).

Since all Cargos experimental fields have the same crop management, we also compared all in-situ measurements and estimations together, obtaining r = 0.3083, p-value = 0.1427, MAE = 0.0439 $cm^3\,cm^{-3}$ and RMSE = 0.0593 $cm^3\,cm^{-3}$ without local calibration and r = 0.5784, p-value = 0.0031, MAE = 0.0559 $cm^3\,cm^{-3}$ and

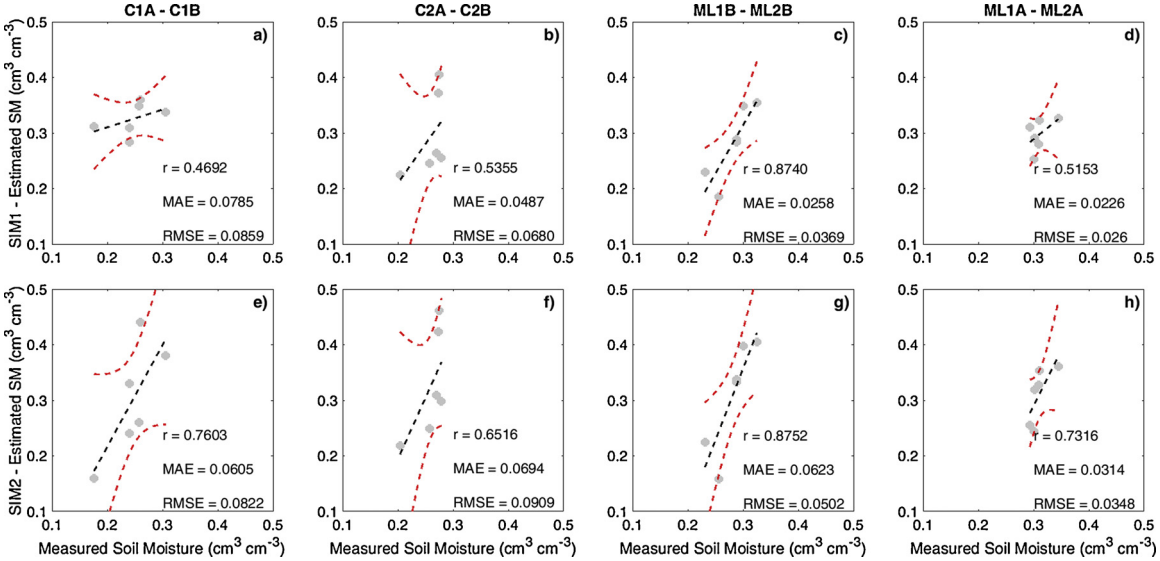

Fig. 6. Estimated versus measured SM from nonlinear OPTRAM for the Cargos plots. The first row (a-d) is based on the Tuscany case study calibration and the second row (e-h) is site specific.

RMSE = 0.077 $cm^3 cm^{-3}$ when applying the site-specific calibration (data not shown). These results confirm that OPTRAM can be universally parameterized for a given location (Sadeghi et al., 2017). A site-specific calibration based on NDVI-STR point cloud distribution enables us to achieve better correlations, although it could lead to higher errors when applied on small fields (in our case around 1 − 2 ha).

The OPTRAM nonlinear parameterization, introduced and applied for the first time for the Tuscany case study and then implemented and applied to the two case studies in Trentino region, provided better accuracy of SM estimations than those calculated by using linear parameterization of wet and dry edge. This is in contrast with the results from Mallik et al. (2009), which show better accuracy of soil moisture estimation for the LST-NDVI based linear parameterization for the dry edge and a horizontal for the wet edge.

Furthermore, in both parameterizations, no oversaturated pixels (above the modeled wet edge in Fig. 2a and Fig. 2b) were detected unlike what was reported by Sadeghi et al. (2017) and Mananze et al. (2019), mainly due to the fact that there are no water body/standing water in our case study. The latter draw attention to a general overestimation of OPTRAM predictions for higher values of soil moisture, particularly for deeper soil level. In this study we observed a slight overestimation in Tuscany with the linear model (on average 0.011 $cm^3 cm^{-3}$), and an overall unbiased prediction with the non linear model. Driest conditions, associated to bare soil immediately after sowing, were slightly underestimated with both models (July 8, 0.14 and 0.11 $cm^3 cm^{-3}$ for non-linear and linear models respectively against 0.23 $cm^3 cm^{-3}$). Overestimations of soil moisture were observed for the Cargos farm. At Agrilife farm, the linear model tends to underestimate SM on rotational grazing pasture (PT) and underestimate high SM values. Overestimations were observed for low soil moisture values on continuous grazing pasture (PC). The nonlinear model instead overestimated soil moisture on PC, while underestimating high SM value and exceed low SM values on PT.

In general, the good correlations between soil moisture measurements and OPTRAM estimations for different soils, sparse or dense crop/vegetation and different management (rainfed and irrigated) can be confirmed, as already highlighted by Sadeghi et al. (2017); Babaeian et al. (2018, 2019) and Mananze et al. (2019). These results were verified across a whole irrigated maize crop season (from sowing to maturity - low to high and saturated NDVI) in Tuscany region with typical dry summer conditions, and in a subalpine zone (Trentino region) where there was a long dry period from late spring to early autumn in 2018 (Climate Change Service, 2018).

3.3. OPTRAM vs. SSM1k product

Fig. 7 presentsSM mean values and standard deviations obtained from nonlinear OPTRAM, SSM1 km and *in situ* measurements for the Tuscany case study. Information on the rainfall events occurring during the examined periods were used as ancillary data. *in situ* measurements, OPTRAM estimated data, and SSM1 km data were available only for three of the dates selected for our study (August 17th, 22nd and 27th). OPTRAM estimations for August 17th and 27th are close to *in situ* measurement values (0.44 ± 0.051 $cm^3 cm^{-3}$ vs. 0.43 $cm^3 cm^{-3}$ and 0.39 ± 0.048 $cm^3 cm^{-3}$ vs. 0.40 $cm^3 cm^{-3}$ respectively) while SSM1 km tends to underestimate the measurements (0.33 and 0.32 $cm^3 cm^{-3}$) for both cases. On August 22nd SSM1 km returns a good estimation of SM (0.416 vs. 0.413 $cm^3 cm^{-3}$) while OPTRAM tends to overestimate the measurement (0.462 ± 0.042 $cm^3 cm^{-3}$). In general, SSM1 km tends to underestimate the *in situ* measurements during maize crop growing season (from July to the end of August) except for the dates following rain events (August 14th and 20th), where a substantial overestimation is observed for those two dates. On the contrary, such a post rainy day (August 8th, 22 mm) overestimation does not occur in the estimate provided by SSM1 km on August 9th, which instead underestimates the *in situ* measurement (0.33 vs. 0.41 $cm^3 cm^{-3}$). For the last period of observations (first half of September) both OPTRAM and SSM1 km tend to slightly overestimate SM measurements. Given that maize sowing date was late in 2018 in Tuscany (June 15th), this bias confirms the seasonal bias reported by Bauer-Marschallinger et al. (2018) and is related to typical indications for vegetation dynamics that superpose the soil water signal. In terms of error, SSM1 km has a double RMSE compared to the nonlinear OPTRAM (0.1264 vs. 0.0619 $cm^3 cm^{-3}$) and also shows a higher error than those reported for SSM1 km validation reports for 6 experimental sites over Europe (Copernicus Global Land Operations, 2018), ranging between 0.033 and 0.093 $cm^3 cm^{-3}$. While a spatial analysis is not feasible because we have only one *in situ* measurement and one SSM1 km pixel, a temporal analysis of SSM1 km and *in situ* SM reveals a low correlation (r = 0.14, data not shown) in agreement again with the results reported by the validation report over Europe (Copernicus Global Land Operations, 2018). It must be noticed that these results are also due to the large difference of scales, in this case comparing information over 1 km with *in situ* point measurement. In fact, if only three dates are considered, a better agreement is found between SSM1 km and nonlinear OPTRAM (r = 0.79, data not shown).

4. Conclusions

In this study, we explored the applicability of Copernicus Sentinel 2 images as a data source for the estimation of surface soil moisture based on the Optical Trapezoid Model (OPTRAM). A linear parameterization of the model was implemented for the Tuscany region case study and soil moisture estimations were compared with in situ measurements for the same area. Pearson's correlation tests showed statistically significant correlations between the observed and estimated soil moisture values; overestimation was observed at medium to high water content levels. A second parameterization considering nonlinear dry and wet edges was performed. The overall better accuracy of the nonlinear model was confirmed by a slight increase in the correlation coefficient and lower RMSE and MAE. Furthermore, when observing the soil moisture maps, the nonlinear model proved to perform better in detecting temporal and spatial soil moisture variability over different environments, crop and vegetation cover, and crop irrigation management.

The practicability of OPTRAM model universal parameterization was confirmed by the results obtained for the Trentino region case study. The soil moisture values obtained underlines the overall better performances of the Tuscany model parameterization over a site-specific model implemented for Trentino. Nevertheless, these affirmations should find further confirmation in other studies exploring the universal parameterization of surface soil moisture estimation models at the site-scale level over different regions. In conclusion, these results indicate that the nonlinear OPTRAM model improves the already promising results from the linear model and further confirm the possibility of an OPTRAM universal parameterization.

Surface soil moisture retrieval from high resolution (10 m) Sentinel 2 images allows detection of water stress situations and supports crop management decision making.

The implementation of such a model can provide useful information in support of agricultural practices giving particular importance when considering irrigation scheduling according to surface soil water content. At the same time, the OPTRAM-SSM1 km data fusion approach should be considered and further explored to overcome the cloud related limitations imposed on Sentinel 2 images exploitation. Ultimately future tests assessing high resolution time series analysis of satellite images for soil moisture retrieval should be considered for longer periods (more seasons) to monitor crop seasonal growth and SSM variability over time.

CRediT authorship contribution statement

Mariapaola Ambrosone: Formal analysis, Writing - original draft,

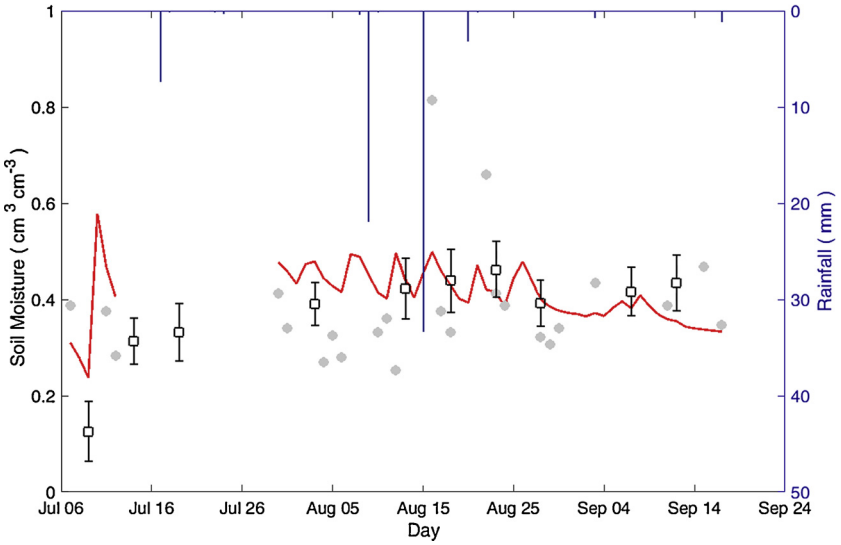

Fig. 7. Rainfall values (mm), SM estimated OPTRAM values (black squares), SM estimated values from 1 km product (gray circles) and *in situ* SM measurements (red line).

Writing - review & editing. **Alessandro Matese:** Methodology, Writing - original draft, Writing - review & editing. **Salvatore Filippo Di Gennaro:** Methodology, Writing - original draft, Writing - review & editing. **Beniamino Gioli:** Writing - original draft, Writing - review & editing. **Marin Tudoroiu:** Investigation, Writing - original draft. **Lorenzo Genesio:** Investigation, Writing - original draft. **Franco Miglietta:** Investigation, Writing - original draft. **Silvia Baronti:** Investigation, Writing - original draft. **Anita Maienza:** Investigation, Writing - original draft. **Fabrizio Ungaro:** Investigation, Writing - original draft. **Piero Toscano:** Conceptualization, Supervision, Methodology, Writing - original draft, Writing - review & editing.

Declaration of Competing Interest

The authors declare that they have no known competing financial interests or personal relationships that could have appeared to influence the work reported in this paper.

Acknowledgements

This work was supported by Agroecological innovations to increase the resilience and sustainability of mountain livestock farms (INVERSION) EIP-AGRI Project, GRANT N.2017IT06RDEI052, 2017-2020.

References

Ahmed, A., Zhang, Y., Nichols, S., 2011. Review and evaluation of remote sensing methods for soil-moisture estimation. J. Photon. Energy 028001–028017. https://doi.org/10.1117/1.3534910.

Avramova, V., Nagel, K.A., Abdelgawad, H., Busto, D., Duplessis, M., Fiorani, F., Beemster, G.T.S., 2016. Screening for drought tolerance of maize hybrids by multi-scale analysis of root and shoot traits at the seedling stage. J. Exp. Bot. 67 (8), 2453–2466. https://doi.org/10.1093/jxb/erw055.

Babaeian, E., Sadeghi, M., Franz, T.E., Jones, S., Tuller, M., 2018. Mapping soil moisture with the OPtical TRApezoid Model (OPTRAM) based on long term MODIS observations. Remote Sens. Environ. 211, 425–440. https://doi.org/10.1016/j.rse.2018.04.29.

Babaeian, E., Sidike, P., Newcomb, M.S., Maimaitijiang, M., White, S.A., Demieville, J., Ward, R.W., Sadeghi, M., LeBauer, D.S., Jones, S.B., Sagan, V., Tuller, M., 2019. A new optical remote sensing technique for high-resolution mapping of soil moisture. Frontiers in Big Data. https://doi.org/10.3389/fdata.2019.00037.

Bauer-Marschallinger, B., Paulik, C., Hochstöger, S., Mistelbauer, T., Modanesi, S., Ciabatta, L., Massari, C., Brocca, L., Wagner, W., 2018. Soil moisture from data fusion of scatterometer and SAR: closing the scale gap with temporal filtering. Remote Sens. (Basel) 10, 1030. https://doi.org/10.3390/rs10071030.

Bosch, D.D., Lakshmi, V., Jackson, T.J., Choid, M., Jacobs, J.M., 2006. Large scale measurements of soil moisture for validation of remotely sensed data: georgia soil moisture experiment of 2003. J. Hydrol. (Amst) 323 (1-4), 120–137. https://doi.org/10.1016/j.jhydrol.2005.08.024.

Campbell, G.S., Norman, J.M., 1988. Introduction to Environmental Biophysics, second ed. Springer edition, USA. https://doi.org/10.1007/978-1-4612-1626-1.

Carlson, T.N., Gillies, R.R., Perry, E.M., 1994. A method to make use of thermal infrared temperature and NDVI measurements to infer surface soil water content and fractional vegetation cover. Remote Sens. Rev. 9 (1-2), 161–173. https://doi.org/10.1080/02757259409532220.

Chan, S.K., Bindlish, R., O'Neill, P.E., Njoku, E., Jackson, T., Colliander, A., Chen, F., Burgin, M., Dunbar, S., Piepmeier, J., et al., 2016. Assessment of the SMAP passive soil moisture product. IEEE T Geosci. Remote 54, 4994–5007. https://doi.org/10.1109/TGRS.2016.2561938.

Chauhan, N.S., 1997. Soil moisture estimation under a vegetation cover: combined active and passive microwave remote sensing approach. Int. J. Remote Sens. 18, 1079–1097. https://doi.org/10.1080/014311603100015683 7.

Chen, T., De Jeu, R.A.M., Liu, Y., Van der Werf, G.R., Dolman, A.J., 2014. Using satellite based soil moisture to quantify the water driven variability in NDVI: a case study over mainland Australia. Remote Sens. Environ. 140, 330–338. https://doi.org/10.1016/j.rse.2013.08.022.

Climate Change Service, 2018. Dry and Warm Spring and Summer. (accessed 01 October 2019). https://climate.copernicus.eu/dry-and-warm-spring-and-summer.

Copernicus Global Land Operations, 2018. Copernicus Global Land Operations. (accessed 01 October 2019). https://land.copernicus.eu/global/sites/cgls.vito.be/files/products/CGLOPS1_VR_SSM1km-V1_I1.20.pdf.

Crow, W.T., Berg, A.A., Cosh, M.H., Loew, A., Mohanty, B.P., Panciera, R., de Rosnay, P., Ryu, D., Walker, J.P., 2012. Upscaling sparse ground-based soil moisture observations for the validation of coarse-resolution satellite soil moisture products. Rev. Geophys. 50 (2). https://doi.org/10.1029/2011RG000372.

Dash, J., Ogutu, B.O., 2016. Recent advances in space-borne optical remote sensing systems for monitoring global terrestrial ecosystems. Prog. Phys. Geog.: Earth and Environment 40 (2), 322–351. https://doi.org/10.1177/0309133316639403.

De Ridder, K., 2000. Quantitative estimation of skin soil moisture with the special sensor microwave/imager. Bound. Lay. Meteorol. 96, 421–432. https://doi.org/10.1023/A:10026686.

Deering, D.W., 1979. Rangeland reflectance characteristics measured by aircraft and spacecraft sensors and spacecraft sensors. Diss. Abstr. Int. B 39, 3081–3082.

Dobson, M.C., Ulaby, F.T., Hallikainen, M.T., El-Rayes, M.A., 1985. Microwave dielectric behavior of wet soil – part II: dielectric mixing models. IEEE T Geosci. Remote 23 (1), 35–46. https://doi.org/10.1109/TGRS.1985.289498.

Doraiswamy, P.C., Hatfield, J.L., Jackson, T.J., Akhmedov, B., Prueger, J., Stern, A., 2004. Crop condition and yield simulations using Landsat and MODIS. Remote Sens. Environ. 92, 548–559. https://doi.org/10.1016/j.rse.2004.05.017.

François, C., 2002. The potential of directional radiometric temperatures for monitoring soil and leaf temperature and soil moisture status. Remote Sens. Environ. 80, 122–133. https://doi.org/10.1016/S0034-4257(01)00293-0.

Gao, H., Wood, E., Drusch, M., Crow, W., Jackson, T., 2004. Using a microwave emission model to estimate soil moisture from ESTAR observations during SGP99. J. Hydrometeorol. 5, 49–63. https://doi.org/10.1175/1525-7541(2004)005<0049:UAMEMT>2.0.CO;2.

Gao, H., Wood, E., Jackson, T., Drusch, M., Bindlish, R., 2006. Using TRMM/TMI to retrieve surface soil moisture over the southern United States from 1998 to 2002. J. Hydrometeorol. 7, 23–38. https://doi.org/10.1175/JHM473.1.

Gillies, R.R., Carlson, T.N., Gui, J., Kustas, W.P., Humes, K., 1997. A verification of the 'triangle' method for obtaining surface soil water content and energy fluxes from remote measurements of the Normalized Difference Vegetation Index (NDVI) and

surface radiant temperature. Int. J. Remote Sens. 18 (15), 3145–3166. https://doi.org/10.1080/014311697217026.
He, B., Xing, M., Bai, X., 2014. A synergistic methodology for soil moisture estimation in an Alpine prairie using radar and optical satellite data. Remote Sens. (Basel) 6, 10966–10985. https://doi.org/10.3390/rs61110966.
IPCC, 2013. In: Stocker, T.F., Qin, D., Plattner, G.-K., Tignor, M., Allen, S.K., Boschung, J., Nauels, A., Xia, Y., Bex, V., Midgley, P.M. (Eds.), Climate Change 2013: The Physical Science Basis. Contribution of Working Group I to the Fifth Assessment Report of the Intergovernmental Panel on Climate Change. Cambridge University Press, Cambridge, United Kingdom and New York, NY. https://doi.org/10.1017/CBO9781107415324. 1535 pp.
IUSS Working Group WRB, 2015. World reference Base for soil resources 2014, update 2015. International Soil Classification System for Creating Legends for Soil Maps. World Soil Resources Reports No. 106. FAO, Rome (accessed 01 October 2019). http://www.fao.org/3/i3794en/I3794en.pdf.
Jackson, T.J., 1993. Measuring surface soil moisture using passive microwave remote sensing. Hydrol. Process. 7, 139–152. https://doi.org/10.1002/hyp.3360070205.
Kerr, Y.H., 2007. Soil moisture from space: where are we? Hydrogeol. J. 15, 117–120. https://doi.org/10.1007/s10040-006-0095-3.
Kerr, Y.H., Waldteufel, P., Richaume, P., Wigneron, J.P., Ferrazzoli, P., Mahmoodi, A., et al., 2012. The SMOS soil moisture retrieval algorithm. IEEE T Geosci. Remote 50 (5), 1384–1403. https://doi.org/10.1109/TGRS.2012.2184548.
Koike, T., Nakamura, Y., Kaihotsu, I., Davva, G., Matsuura, N., Tamagawa, K., 2004. Development of an advanced microwave scanning radiometer (amsre) algorithm of soil moisture and vegetation water content. Annu. J. Hydraul. Eng., Jpn. Soc. Civil Eng 48, 217–222. https://doi.org/10.2208/prohe.48.217.
Kubelka, P., Munk, F., 1931. An Article on Optics of Paint Layers. (accessed 01 October 2019). http://www.graphics.cornell.edu/-westin/pubs/kubelka.pdf.
Lakhankar, T., Krakauer, N., Khanbilvardi, R., 2009. Applications of microwave remote sensing of soil moisture for agricultural applications. Int. J. Terraspace Sci. Eng. 2 (1), 81–91 Doi:10.1.1.701.7873.
Lakshmi, V., 2012. Remote sensing of soil moisture. ISRN Soil Sci. 2013, 424178. https://doi.org/10.1155/2013/424178.
Lambin, E.F., Ehrlich, D., 1996. The surface temperature – vegetation index space for land cover and land-cover change analysis. Int. J. Remote Sens. 17, 463–487. https://doi.org/10.1080/01431169608949021.
Liu, S., Roberts, D.A., Chadwick, O.A., Still, C.A., 2012. Spectral response to plant available soil moisture in a Californian grassland. Int. J. Appl. Earth Obs. 19, 31–44. https://doi.org/10.1016/j.jag.2012.04.008.
Magagi, R., Kerr, Y., Wigneron, J.-P., 2016. 2 - Estimation of soil Water conditions using passive microwave remote sensing. In: Baghdadi, N., Zribi, M. (Eds.), Land SUrface Remote Sensing in Continental Hydrology. Elsevier, pp. 41–78. https://doi.org/10.1016/B978-1-78548-104-8.50002-4.
Mallick, K., Bhattacharya, B.K., Patel, N.K., 2009. Estimating volumetric surface moisture content for cropped soils using a soil wetness index based on surface temperature and NDVI. Agr. Forest Meteorol. 149 (8), 1327–1342. https://doi.org/10.1016/j.agrformet.2009.03.004.
Mananze, S., Pôças, I., Cunha, M., 2019. Agricultural drought monitoring based on soil moisture derived from the optical trapezoid model in Mozambique. J. Appl. Remote Sens. 13 (2), 1–16. https://doi.org/10.1117/1.JRS.13.024519.
Mathworks Inc, 2016. MATLAB And Statistics Toolbox Release. https://doi.org/2016-11-26. www.mathworks.com/products/matlab.
McCabe, M., Wood, E., Gao, H., 2005. Initial soil moisture retrievals from AMSRT-E: multiscale comparison using in situ data and rainfall patterns over Iowa. Geophys. Res. Lett. 32, L06403. https://doi.org/10.1029/2004GL021222.
Moran, M.S., Peters-Lidard, C.D., Watts, J.M., McElroy, S., 2004. Estimating soil moisture at the watershed scale with satellite-based radar and land surface models. Can. J. Remote Sens. 30, 805–826. https://doi.org/10.5589/m04-043.
Mulder, V.L., de Bruin, S., Schaepman, M.E., Mayr, T.R., 2011. The use of remote sensing in soil and terrain mapping – a review. Geoderma 162, 1–19. https://doi.org/10.1016/j.geoderma.2010.12.018.
Nemani, R., Pierce, L., Running, S., Goward, S., 1993. Developing satellite-derived estimates of surface moisture status. J. Appl. Meteorol. Climatol. 32 (3), 548–557. https://doi.org/10.1175/1520-0450(1993)032%3C0548:DSDEOS%3E2.0.CO;2.
Njoku, E.G., Kong, J.A., 1977. Theory for passive microwave remote sensing of near surface soil moisture. J. Geophys. Res. 82 (20), 3108–3118. https://doi.org/10.1029/JB082i020p03108.
Njoku, E., Li, L., 1999. Retrieval of land surface parameters using passive microwave measurements at 6-18 GHz. IEEE Trans. Geosci. Remote Sens. 37, 79–93. https://doi.org/10.1109/36.739125.
Njoku, E., Jackson, T., Lakshmi, V., Chan, T., Nghiem, S., 2003. Soil moisture retrieval from AMSR-E. IEEE T Geosci. Remote 41 (2), 215–229. https://doi.org/10.1109/TGRS.2002.808243.
Owe, M., de Jeu, R., Walker, J., 2001. A methodology for surface soil moisture and vegetation optical depth retrieval using the microwave polarization difference index. IEEE Trans. Geosci. Remote Sens. 39, 1643–1654. https://doi.org/10.1109/36.942542.
Paloscia, S., Santi, E., Pettinato, S., Mladenova, I., Jackson, T., Bindlish, R., Cosh, M., 2015. A comparison between two algorithms for the retrieval of soil moisture using AMSR-E data. Front. Earth Sci. 3 (16). https://doi.org/10.3389/feart.2015.00016.
Pan, M., Sahoo, A.K., Wood, E.F., 2014. Improving soil moisture retrievals from a physically-based radiative transfer model. Remote Sens. Environ. 140, 130–140. https://doi.org/10.1016/j.rse.2013.08.020.
Paulik, C., Dorigo, W., Wagner, W., Kidd, R., 2014. Validation of the ASCAT Soil Water Index using in situ data from the International Soil Moisture network. Int. J. Appl. Earth Obs. 30, 1–8. https://doi.org/10.1016/j.jag.2014.01.007.
Peng, J., Loew, A., Merlin, O., Verhoest, N., 2017. A review of methods for downscaling remotely sensed soil moisture. Rev. Geophys. 55, 341–366. https://doi.org/10.1002/2016RG000543.
Piles, M., Camps, A., Vall-llossera, M., Corbella, I., Panciera, R., Rudiger, C., Kerr, Y.H., Walker, J., 2011. Downscaling SMOS derived soil moisture using MODIS visible/infrared data. IEEE T Geosci. Remote 49 (9), 3156–3166. https://doi.org/10.1109/TGRS.2011.2120615.
R Core Team, 2019. R: a Language and Environment for Statistical Computing. URL. R Foundation for Statistical Computing, Vienna, Austria. https://www.R-project.org/.
Rahimzadeh, P., Berg, A., 2016. Chapter 3- soil moisture retrievals using Optical/TIR methods. J.Satel.Soil Mois.Retrival 47–72. https://doi.org/10.1016/B978-0-12-803388-3.00003-6.
Sadeghi, A.M., Jones, S.B., Philpot, W.D., 2015. A linear physically – based model for remote sensing of soil moisture using short wave infrared bands. Remote Sens. Environ. 164, 66–76. https://doi.org/10.1016/j.rse.2015.04.007.
Sadeghi, M., Babaeian, E., Tuller, M., Jones, S.B., 2017. The optical trapezoid model: a novel approach to remote sensing of soil moisture applied to Sentinel-2 and Landsat-8 observations. Remote Sens. Environ. 198, 52–68. https://doi.org/10.1016/j.rse.2017.05.041.
Santos, W.J.R., Silva, B.M., Oliveira, G.C., Volpato, M.M.L., Lima, J.M., Curi, N., Marques, J.J., 2014. Soil moisture in the root zone and its relation to plant vigor assessed by remote sensing at management scale. Geoderma 221-222, 91–95. https://doi.org/10.1016/j.geoderma.2014.01.006.
Şekertekin, A., Marangoz, A.M., Abdikan, S., 2016. Soil moisture mapping using Sentinel-1A synthetic aperture radar data. Int. J. Environ. Geoinformatics. 5 (2), 178–188. https://doi.org/10.30897/ijegeo.
Sobrino, J.A., Franch, B., Mattar, C., Jiménez-Muñoz, J.C., Corbari, C., 2012. A method toestimate soil moisture from Airborne Hyperspectral Scanner (AHS) and ASTER data:application to SEN2FLEX and SEN3EXP campaigns. Remote Sens. Environ. https://doi.org/10.1016/j.rse.2011.10.018.
Thoma, D.P., Moran, M.S., Bryant, R., Rahman, M.M., Collins, C.D.H., Keefer, T.O., Noriega, R., Osman, I., Skrivin, S.M., Tischler, M.A., Bosch, D.D., Peters-Lidard, C.D., 2008. Appropriate scale of soil moisture retrieval from high resolution radar imagery for bare and minimally vegetated soils. Remote Sens. Environ. 112 (2), 403–414. https://doi.org/10.1016/j.rse.2007.06.021.
Tollenaar, M., Lee, E.A., 2002. Yield potential, yield stability and stress tolerance in maize. Field Crops Res. 75, 161–169. https://doi.org/10.1016/S0378-4290(02)00024-2.
Ulaby, F.T., Dubois, P.C., Van Zyl, J., 1996. Radar mapping of surface soil moisture. J. Hydrol. (Amst) 184, 57–84. https://doi.org/10.1016/0022-1694(95)02968-0.
Umar, M., Munir, S., Ali, I., Qureshi, S., Notarnicola, C., Rahman, S., Weng, Q., 2016. Soil moisture using optical remote sensing and ground measurements. A case study from Pakistan. In: Weng, Q. (Ed.), Remote Sensing for Sustainability. Pub. Location Boca Raton. https://doi.org/10.1201/9781315371931. chapter 13. Edited by.
Vanino, S., Nino, P., De Michele, C., Falanga Bolognesi, S., D'Urso, G., Di Bene, C., Pennelli, B., Vuolo, F., Farina, R., Pulighe, G., Napoli, R., 2018. Capability of Sentinel-2 data for estimating maximum evapotranspiration and irrigation requirements for tomato crop in Central Italy. Remote Sens. Environ. 215, 452–470. https://doi.org/10.1016/j.rse.2018.06.035.
Vuolo, F., D'Urso, G., De Michele, C., Bianchi, B., Cutting, M., 2015. Satellite-based irrigation advisory services: a common tool for different experiences from Europe to Australia. Agr. Water Manage. 147, 82–95. https://doi.org/10.1016/j.agwat.2014.08.004.
Wagner, W., Lemoine, G., Rott, H., 1999. A method for estimating soil moisture from ERS scatterometer and soil data. Remote Sens. Environ. 70 (2), 191–207. https://doi.org/10.1016/S0034-4257(99)00036-X.
Wang, X., Xie, H., Guan, H., Zhou, X., 2007. Different responses of MODIS derived NDVI to root zone soil moisture in semi-arid and humid regions. J. Hydrol. (Amst) 340 (1-2), 12–24. https://doi.org/10.1016/j.jhydrol.2007.03.022.
WWAP (United Nations World Water Assessment Programme), 2015. The United Nations World Water Development Report 2015: Water for a Sustainable World. UNESCO, Paris (accessed 01 October 2019). http://unesdoc.unesco.org/images/0023/002318/231823E.pdf.
Zhang, D., Zhou, G., 2016. Estimation of soil moisture from optical and thermal remote sensing: a review. Sensors 16, 1308. https://doi.org/10.3390/s16081308.